Environmental Science & Technology

Article

pubs.acs.org/est

Mercury Localization and Speciation in Plants Grown Hydroponically or in a Natural Environment

Sandra Carrasco-Gil,[*,‡,§,†] Hagar Siebner,[∥,†,¶] Danika L. LeDuc,[⊥] Samuel M. Webb,[#] Rocío Millán,[§] Joy C. Andrews,[⊥,#] and Luis E. Hernández[‡]

[‡]Laboratory of Plant Physiology, Department of Biology, Universidad Autónoma de Madrid, 28049 Madrid, Spain

[§]Centro de Investigaciones Energéticas, Medioambientales y Tecnológicas, Avd. Complutense, 22, 28040 Madrid, Spain

[∥]Department of Geological and Environmental Sciences, Stanford University, 367 Panama St., Stanford, California 94305-2115, United States

[⊥]Department of Chemistry and Biochemistry, California State University, East Bay 25800 Carlos Bee Boulevard, Hayward, CA

[#]Stanford Synchrotron Radiation Lightsource, 2575 Sand Hill Road, SLAC MS 69 Menlo Park, CA

Supporting Information

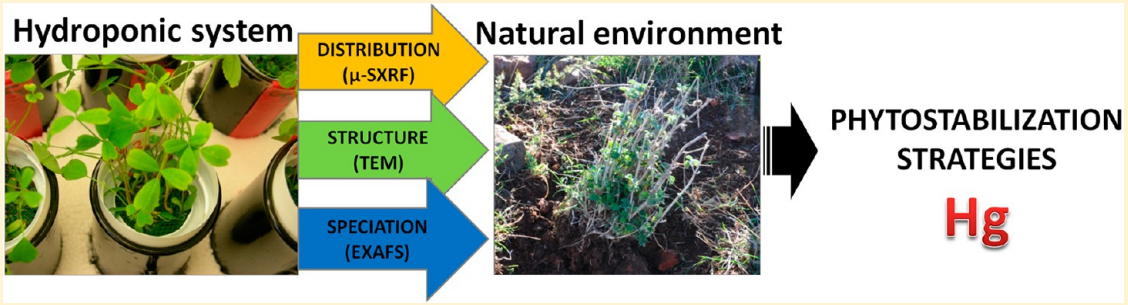

ABSTRACT: Better understanding of mercury (Hg) accumulation, distribution, and speciation in plants is required to evaluate potential risks for the environment and to optimize phytostabilization strategies for Hg-contaminated soils. The behavior of Hg in alfalfa (*Medicago sativa*) plants grown under controlled conditions in a hydroponic system (30 μM $HgCl_2$) was compared with that of naturally occurring Horehound (*Marrubium vulgare*) plants collected from a mining soil polluted with Hg (Almadenejos, Spain) to characterize common mechanisms of tolerance. Synchrotron X-ray Fluorescence microprobe (μ-SXRF) showed that Hg accumulated at the root apex of alfalfa and was distributed through the vascular system to the leaves. Transmission electron microscopy (TEM) implied association of Hg with cell walls, accompanied by their structural changes, in alfalfa roots. Extended X-ray absorption fine structure (EXAFS) determined that Hg was principally bound to biothiols and/or proteins in *M. sativa* roots, stems, and leaves. However, the major fraction of Hg detected in *M. vulgare* plants consisted of mineral species, possibly associated with soil components. Interestingly, the fraction of Hg bound to biothiols/proteins (i.e., metabolically processed Hg) in leaves of both plants (alfalfa and *M. vulgare*) was similar, in spite of the big difference in Hg accumulation in roots, suggesting that some tolerance mechanisms might be shared.

INTRODUCTION

Mercury is highly toxic to humans and ecosystems and is considered a global pollutant because it is highly mobile and extremely persistent in the environment.[1] The occurrence of heavily Hg-polluted soils is frequently associated with natural deposition, which is derived from the weathering of Hg-containing bedrock minerals, and anthropogenic dispersion from mining and smelting activities as is the case for Hg in the mining Almadén district, Spain.[2] In such areas, the phytostabilization of pollutants using the innate properties of plants to accumulate them in below ground organs might be the most feasible phytoremediation strategy to use, creating a vegetation cover to limit Hg dispersion in the environment.[3] In addition, Hg uptake by aboveground organs increases the risk of its entry to the food chain; a problem aggravated by agricultural practices performed in the surroundings of abandoned mines and smelting facilities.[4]

Mercury can be found in the environment in several forms including the monatomic metallic form (Hg^0), ionic Hg (Hg^+, Hg^{2+}) as a component of metal ores (e.g., in cinnabar; HgS), or in methylated forms (CH_3Hg^+, $(CH_3)_2Hg$), which cause the highest toxic effect in humans.[5] Depending on environmental conditions, Hg might also undergo transformations, generally through reduction or methylation/demethylation,[6,7] affecting its toxicity and distribution in the environment. Exposure to

Received: August 15, 2012
Revised: December 22, 2012
Accepted: February 13, 2013
Published: February 13, 2013

 © 2013 American Chemical Society

methyl-Hg may also occur in some crops cultivated under anoxic (flooded) conditions, such as rice.[8,9]

Characterization of the distribution and speciation of toxic metals in plants is fundamental to the understanding of accumulation and transport mechanisms,[10,11] which in turn would help to optimize plant performance in phytostabilization strategies.[12] These mechanisms are regulated by several physiological processes including transport of metals across the plasma membrane of root cells, detoxification, and sequestration of metals in vacuole or cell walls, xylem loading, and translocation from root to shoot.[13] In this respect, little is known about the speciation of Hg in plants and how it is distributed at the tissular and cellular levels.

Spatially resolved synchrotron source X-ray spectroscopy can provide key knowledge about uptake, transport, and storage of essential and nonessential metals by plants.[14,15] Concretely, synchrotron X-ray fluorescence (μ-SXRF) is capable of providing very good spatial resolution (typically few micrometers), and is very sensitive (usually >10 ppm), depending on beamline capabilities, metal type, and chemical environment (comprehensive review by Lombi et al.).[16] With regard to Hg in plants, only a few studies have been published so far referring to its localization at the tissue and cellular levels: De Filippies and Pallaghy[17] used scanning electron microscopy (SEM) coupled with energy dispersive X-ray analysis (EDXA) to localize Hg at the cellular level in *Hordeum vulgare* root cells and found that Hg was mainly accumulated within the nucleus. Patty et al.[18] used μ-SXRF mapping and transmission X-ray microscopy (TXM) imaging in *Spartina* spp. and showed that the highest concentration of Hg in young roots was localized at the apical area and inner tissues. Carrasco-Gil et al.[19] used μ-SXRF and fluorescence μ-tomography in *Medicago sativa* roots grown in a hydroponic system and observed high Hg accumulation at the epidermis and the vascular cylinder of mature roots with a weaker accumulation in the endodermis. A recent study described diverse distribution patterns of Hg in roots of shrubs growing on Hg-mine wastes depending on plant species, developmental stage and environmental conditions.[20]

Besides spatial distribution, a synchrotron light source may provide detailed information with respect to the metal speciation; characterizing the chemical coordination environments of the metal binding sites in the sample using extended X-ray absorption fine structure (EXAFS) and X-ray absorption near edge structure (XANES). Riddle et al.[21] concluded that Hg in roots could be bound ionically, most likely to carboxylate groups of organic acids, but covalently to sulfur groups in shoots. However, Rajan et al.[22] and Patty et al.[18] found that Hg was mostly bound to S-containing ligands in roots. This was also the case with *M. sativa* roots, where most soluble Hg was found to associate with cysteine residues, and the plants were found to accumulate an array of Hg−phytochelatin (Hg−PCs) complexes.[19] According to a subcellular fractionation, Hg was mostly associated with cell walls in *M. sativa* and *Halimione portulacoides* plants.[19,23] These studies did not detail distribution and speciation of Hg in above ground tissues (i.e., stems and leaves).

Metal distribution and speciation in plants are often studied in hydroponic systems under homogeneous and controlled environmental conditions, employing high concentrations to ease detection of the metal. This is in opposition to field experiments, characterized by high heterogeneity and relatively low metal levels, often at the detection limit of the analytical methods. In this study, we implemented the same analytical methodology on two different Hg contaminated systems: (1) alfalfa (*Medicago sativa*, cv. Aragon) grown under hydroponic conditions and high Hg concentration, and (2) Horehound (*Marrubium vulgare* L., Lamiaceae), which grows naturally in arid soils, highly polluted with Hg in the Almadén area, Ciudad Real, Spain.[24] This mining site constitutes the largest natural deposit of Hg in the world, where Hg is found mainly as cinnabar.[4] Despite the fact that most Hg is found as cinnabar (which has relatively low solubility) in these soils, a significant concentration of the metal can be found in the local plants.[25,24] We have studied these two diverse plant systems using synchrotron X-ray methods and TEM to determine differences and similarities in Hg uptake and transformation, for potential application to phytostabilization strategies.

EXPERIMENTAL METHODS

Plant Material. *Medicago sativa* (alfalfa) seedlings were grown in a pure hydroponic system with continuous aeration in a controlled environment chamber as previously described.[19,26] The plants grew for 12 days in control solution (see Supporting Information for details) and then were treated with 30 μM Hg (as $HgCl_2$) from 5 h to 7 days. The metal dosage (equal to 6 μg mL^{-1}) was chosen to match the level of Hg available in polluted soils of the area of interest,[27,28] still high enough to enable reliable measurements. The Hg^{2+} concentration in the nutrient solution was confirmed in silico using *Visual MINTEQ 3.0* chemical speciation software with Lindsaý's databases.[29]

For naturally grown *Marrubium vulgare*, 12 plants were collected from an abandoned metallurgical plant located in Almadenejos (12 km SE of Almadén, Cuidad Real, Spain). Four samples were collected at each of the three sampling points (P1, P2, and P3 in Figure S2 of the Supporting Information). Plants were thoroughly washed with deionized water to remove superficial Hg. In addition, an ultrasonic bath treatment (Ultrasons-H, Selecta, Barcelona, Spain; 3 cycles of 10 min) was applied to *M. vulgare* plants to remove soil particles. A representative portion was frozen (−80 °C) for EXAFS analysis.

Total Hg Concentration in Plants. *M. sativa and M. vulgare* samples were air-dried and ground to homogeneity with mortar and pestle. Dried sample (100 mg) was acid digested as described by Ortega-Villasante et al.,[30] and Hg concentration was measured as described in Carrasco-Gil et al.[19]

Synchrotron X-ray Fluorescence Microprobe (μ-SXRF). Samples were embedded in Epo-Tek 301−2FL to preserve their structure because tissues of Hg-treated plants were very delicate and tended to collapse. Cross sections of *M. sativa* and *M. vulgare* roots were analyzed by microprobe at the Stanford Synchrotron Radiation Lightsource (SSRL) beamline 2−3. The Data analysis was carried out with the MicroAnalysis Toolkit (SMAK, version 0.50).[31] Further information regarding sample preparation and technical data is provided in the Supporting Information.

Transmission X-ray Microscopy (TXM). Thin sections (60 μm) were prepared following the procedure described above for μ-SXRF. A cross section of *M. vulgare* root sampled at spot P2 (Figure S2 of the Supporting Information) was scanned with the X-ray microscope at SSRL beamline 6−2. See the Supporting Information for details.

Transmission Electron Microscopy (TEM). Root samples of *M. sativa* (ca. 5 mm from the tip of a primary root) were fixed and embedded according to Russin and Trivett[32] with the following modification: samples were not counterstained with

Table 1. Total Hg Concentrations (μg g^{-1} DW) in the Organs of *M. sativa* and *M. vulgare* Plants[a]

	M. sativa (Hydroponic)		*M. vulgare* (Hg-Polluted Sites)		
	30 μM Hg	control	P1	P2	P3
roots	2,611.0 ± 273.0	NA	36.7 ± 0.7	203.5 ± 4.7	501.9 ± 3.2
stems	38.3 ± 0.45	2.0 ± 0.5			
leaves	67.7 ± 0.5	8.0 ± 2.2	32.8 ± 1.0	60.7 ± 8.7	183.4 ± 7.1
soil (T)[b]			678 ± 42	3358 ± 417	7862 ± 1595
soil (A)[b]			0.04–0.37	0.11–0.78	0.7–15.8
soil (A)[c]				10.8–21.3	

[a]Data are average of three independent assays (±SD) for *M. sativa* and four independent samples (±SD) for *M. vulgare*. Total Hg (T) (μg g^{-1} DW) and available Hg (A) (μg mL^{-1}) concentration in the Hg-contaminated soil from Almadenejos. [b]Millán et al., 2011. [c]Esbrí et al., 2010.

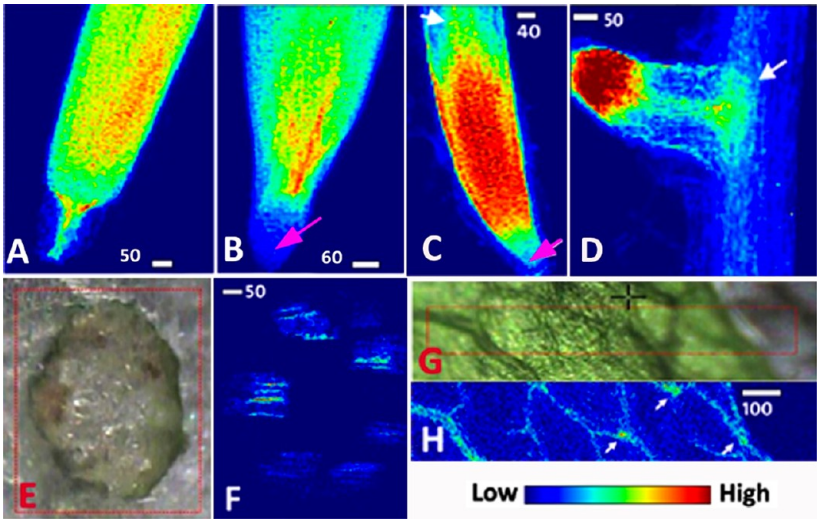

Figure 1. μ-SXRF Hg map of *M. sativa* treated with 30 μM Hg in a pure hydroponic system. Primary roots treated for 5 h (**A**), 24 h (**B**), and 7 days (**C**). Secondary root tip treated for 7 days (**D**). Stem (**F**) and leaf (**H**) of plants treated for 7 days. The red square in the optical images of stem (**E**) and leaf (**G**) shows the region selected for μ-SXRF imaging (scale bar is in μm).

other heavy metals (i.e., lead, uranium or osmium; as conventionally performed to reveal cellular details). Under these conditions, it is reasonable to assume that electron dense deposits that appeared in Hg-treated root samples and absent in the parallel control samples imply metal deposit formation. A similar approach was recently described by Sanità di Toppi et al.[33] in Cd-treated carrot roots. Ultrathin sections (90 nm) were cut and scanned with a TEM microscope to follow both electron-dense deposits and structural effects of Hg-treatment. See the Supporting Information for more details.

Extended X-ray Absorption Fine Structure (EXAFS). Reference compounds representing the most probable Hg coordination environments in plants were chosen: inorganic sulfur bonding (cinnabar, Hg–S red; and *meta*cinnabar, Hg–S black), organic sulfur bonding to sulfides (phytochelatins, Hg–PCs; glutathione, Hg–GSH; cysteine, Hg–Cys), and to thioether (methionine, Hg–Met), oxygen bonding (acetate, Hg–Ace; and montroydite, HgO), and methyl-Hg forms (CH_3–Hg–cysteine, CH_3–Hg–aspartate and CH_3–Hg–methionine), as well as Hg bound to the nonpolar amino acid alanine (Hg–Ala); and $HgCl_2$, which was the Hg source in the hydroponic nutrient solution. Reference standards were prepared following the procedure described by Carrasco-Gil et al.[19] and Rajan et al.[22] and were used for fit calculations. Fresh *M. sativa* samples were ground and stored at −80 °C. Freeze-dried *M. vulgare* samples were ground and stored at room temperature until analysis. Hg L_3 X-ray absorption spectra for the hydroponic *M. sativa* root (average of 4 scans), stem (average of 25 scans), and leaf (average of 16 scans); and *M. vulgare* root and leaf (average of 20 scans) were collected at beamline 11–2 at SSRL (Supporting Information for beamline setup). Data analysis was carried out following the procedure described by Carrasco-Gil et al.[19] using *SixPACK* software package, version 0.68.[34] The fingerprinting method was used to quantify the percentage of each Hg species present in *M. sativa* and *M. vulgare* organs; a least-squares fit (LSF) was performed to fit the EXAFS (*chi*) of the experimental data to linear combinations of the above-mentioned standard reference compounds. Selected candidates with a significant contribution (>10%)[35] were fitted to get the relative proportion of Hg species. The quality of the fit was evaluated by R-factor as described by Kelly et al.[36]

RESULTS

Plant Growth and Total Hg Concentration. Significant inhibition of growth was observed in *M. sativa* roots and shoots, measured as organ length and fresh weight of plants treated with 30 μM Hg (part B of Figure S1 of the Supporting Information). Some visual symptoms of toxicity appeared as minor leaf chlorosis (part A of Figure S1 of the Supporting Information). There was a remarkable increase in total Hg concentration in treated plants (Table 1), which was particularly high in the roots and much lower in leaves (ca. 2 orders of magnitude). We could observe a minor contamination

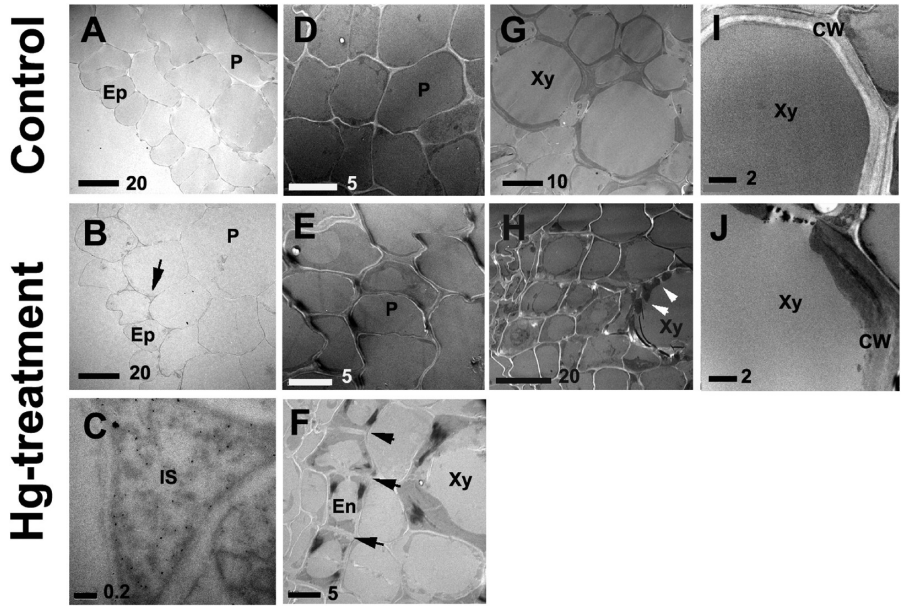

Figure 2. Transmission electron microscopy of a cross section in *M. sativa* primary root treated with 0 μM Hg (control) and 30 μM Hg for 7 days (Hg-treated). TEM images show the absence or presence of dark electron-dense spots corresponding to Hg accumulation in different tissues and the resulting structural changes. Epidermal and external cortical cells (**A**–**C**): Control (**A**); dark spots in the intercellular spaces of the external layers of the root, between epidermal and cortical cells of Hg-treated plants (**B**); magnification of an intercellular space (marked with arrow in B) containing granular deposits of Hg (**C**). Cortical cells (**D**–**E**): control (**D**), Hg-treated root (**E**); endodermal cells (arrows indicate Casparian stripes) (**F**). Vascular cylinder cells (**G**–**J**): control (**G**), vs Hg-treated root (**H**); white arrows indicate faults in cell wall; magnification of a xylem vessel in control (**I**); and Hg-treated root (**J**). Ep, epidermis; IS, intercellular space; P, parenchyma; En, endodermis; CW, cell wall; Xy, xylem.

of Hg in control shoots possibly caused by volatilization from the neighboring Hg-containing nutrient solution.

The concentration of Hg in *M. vulgare* plants collected from Hg-polluted sites in Almadén increased from sampling point P1 to point P3 (Table 1), following the soil and atmospheric Hg concentration gradient at these points[28,37] (part A of Figure S2 of the Supporting Information). Mercury levels in roots were higher than in shoots. Despite the high concentration of Hg, these plants did not display visual symptoms of toxicity.

Localization of Hg in *Medicago sativa*. μ-SXRF analysis was performed in alfalfa plants grown in controlled environmental conditions and treated with 30 μM Hg for different time intervals. Mercury rapidly accumulated at the root tip after 5 h of exposure (part A of Figure 1). After 24 h, the Hg signal was concentrated in the inner tissues behind the meristem (part B of Figure 1). A long-term exposure treatment of 30 μM Hg for 7 d revealed that Hg was still accumulated in the apical region of primary and secondary roots as well as in the vascular cylinder and the epidermis (parts C and D of Figure 1), although the intensity decreased with the distance from the tip (upper white arrows in parts C and D of Figure 1).

Transmission electron microscopy (TEM) was used to localize Hg at the tissular and cellular level in root sections of *M. sativa*, treated with 30 μMHg for 7 days. Granular deposits were observed only in Hg-treated root sections at the intercellular space, between the epidermis and the external layers of the cortex (parts B and C of Figure 2) and were completely absent in control root sections (part A of Figure 2). Cortex cells were deformed in Hg-treated plants, and showed uneven structures (compare parts D and E of Figure 2). Specific dense deposits were also found in non suberized areas of the endodermis (black arrows mark suberized areas of Casparian strip, part F of Figure 2). A strong effect of Hg was also observed in the vascular cylinder; where the cell walls of xylem vessels were thicker, uneven and contained many openings and faults, in comparison with smooth uniform cell walls of control roots (compare Hg-treated samples parts H, J, and F of Figure 2 with the control in parts G and I of Figure 2).

μ-SXRF scans of stem cross sections showed that Hg signal was located in circular areas corresponding with vascular bundles (part F of Figure 1). The spatial resolution and mechanical damage during cutting (due to reduced firmness of samples from Hg-treated plants) did not enable discrimination between phloem and xylem, which are packed together in these bundles. In leaves, Hg could also be observed in the veins (part H of Figure 1).

Localization of Hg in *Marrubium vulgare*. The spatial localization of Hg in naturally grown plants was studied by μ-SXRF in cross sections of *M. vulgare* roots collected from the P2 contaminated plot in Almadén (part A of Figure S2 of the Supporting Information). The most intense Hg signal in roots was found at the root external layers (part B of Figure 4). Mercury was not detected in inner tissues of the root, except for a small area (marked with arrow in part B of Figure 4) and few hot spots. A mosaic TXM image of a delimited cross section area also showed dark contrasted areas mainly in the root perimeter (part C of Figure 4). It also showed a dark particle, seated on the boundary of the vascular cylinder, which was colocalized with the hot spot of Hg in the μ-SXRF image in part B of Figure 4. Though noisy, the oscillations and peak ratios of the μ-EXAFS spectrum of this particular hot spot implied that it consisted mainly of cinnabar (90% by LSF, R-factor = 0.549).

An effort was made to localize Hg in *M. vulgare* leaves and stems as well. However, the μ-SXRF images of Hg showed an inconsistent distribution pattern in different tissues (data not shown), probably caused by the low Hg concentration, near the detection limit of the beamline used, and the characteristic

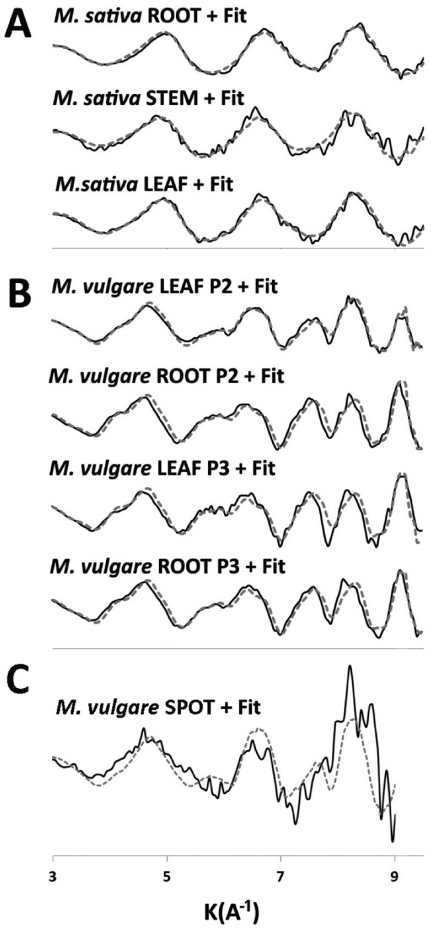

Figure 3. Hg L_3 EXAFS k^3 weighted spectrum (solid black line) and the linear combination fit (dashed gray line) of root, stem and leaf of *M. sativa* (**A**); roots and leaves of *M. vulgare* sampled at points P2 and P3 (**B**); and μ-EXAFS spectrum collected at Hg hot spot (marked with number 1 in part B of Figure 4) (**C**).

highly corrugated leaf anatomy of this plant species, with abundant hairs and trichomes.

Bulk Hg Speciation in *Medicago sativa* and *Marrubium vulgare*. The bulk chemical speciation of Hg in *M. sativa* (root, stem, and leaf) as well as *M. vulgare* (root and leaf) was investigated by Hg L_3-edge EXAFS spectroscopy. Complexes of Hg with the different PCs and GSH were indistinguishable at the signal-to-noise ratio of the samples; thus, we opted to use Hg–hPC_2 as a representative standard for this group (Hg–PCs). For a similar reason, we chose HgCys to represent Hg–cysteine complexes (including proteins) and CH_3HgAsp as representative of methylated Hg forms (CH_3–Hg). The EXAFS spectra of the selected reference compounds are presented in Figure S3 of the Supporting Information.

The EXAFS spectra and results of the LSF of Hg species for the hydroponically grown *M. sativa* plants are presented in part A of Figure 3 and summarized in Table 2. The LSF analysis found that organic Hg–S species (i.e., biothiols, including Hg–PC and Hg–Cys) were the dominant Hg forms in *M. sativa* roots, comprising 77% of Hg species (Table 2). These species also constituted the major proportion in leaves (73%) and stems (100%). A smaller, yet significant, fraction of Hg (>20%) was found in methylated forms (CH_3–Hg, Table 2). No inorganic forms and minerals of Hg were detected in *M. sativa* tissues.

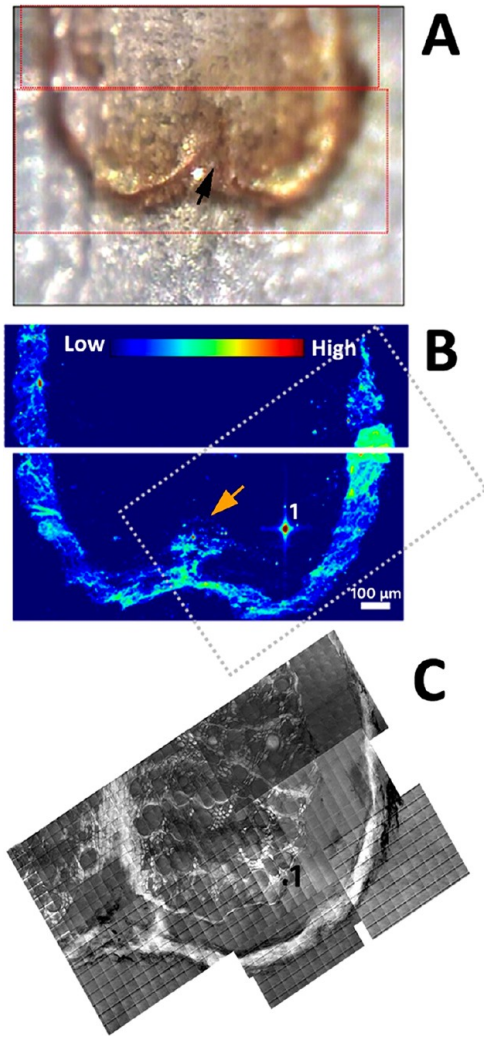

Figure 4. Distribution of Hg in a root cross section of *Marrubium vulgare* grown in an abandoned metallurgic plot. Optical image (arrow points to a fracture in the root) (**A**); X-ray fluorescence (μ-SXRF) map showing Hg distribution (orange arrow indicates an intrusion of outer layer) (**B**); TXM mosaic image shows dark areas due to the absorption by Hg (**C**); red rectangles in (A) represent the mapped area in μ-SXRF image, and the gray rectangle in (B) represents the mapped area in TXM image. Number 1 in (B) and (C) refers to the position where μ-EXAFS was collected.

The EXAFS spectra and LSF analysis of *M. vulgare* plants, collected from contaminated sampling points P2 and P3, are presented in part B of Figure 3 and Table 2 (Hg concentrations in P1 samples were low, resulting in noisy spectra that were not further analyzed). The major forms of Hg found in roots and leaves of *M. vulgare* were HgS minerals; cinnabar, and metacinnabar (58–83%, Table 2). A smaller proportion was bound to biothiols/proteins in Hg–PC and Hg–Cys (12–42%). The organic CH_3–Hg forms were detected only in roots of *M. vulgare*, but this fraction was at the limit of method sensitivity (10%).

DISCUSSION

Mercury accumulated to a higher extent in roots than in the aerial parts of the plants, both in *M. sativa* grown hydroponically or in naturally occurring *M. vulgare* collected from a polluted soil. Similar results were reported in plants grown

dx.doi.org/10.1021/es303310t | *Environ. Sci. Technol.* 2013, 47, 3082–3090

Table 2. Relative Proportion (%) of Mercury (Hg) Species in: Three-Week-Old *M. sativa* Root Treated with 30 μM Hg for 7 days; *M. vulgare* Collected from Two Different Points (P3 and P2) in an Abandoned Metallurgical Plant; and the Hot Spot of *M. vulgare* Root[a]

	M. sativa			*M. vulgare*				
	root	stem	leaf	root P2	leaf P2	root P3	leaf P3	root spot 1
Hg−PC (%)	43 ± 3	83 ± 8	14 ± 4	19 ± 6	12 ± 3		17 ± 3	
Hg−Cys ligand (%)	34 ± 4	17 ± 8	59 ± 4		30 ± 4	12 ± 5		
Hg−S red (%)				19 ± 4	30 ± 2	32 ± 4	28 ± 4	90 ± 4
Hg−S black (%)				52 ± 2	28 ± 1	46 ± 2	55 ± 2	
CH_3−Hg (%)	23 ± 2		27 ± 2	10 ± 4		10 ± 4		
R-factor	0.053	0.159	0.060	0.167	0.099	0.108	0.170	0.549

[a]Best fits using Least-Square-Fitting (LSF) of Hg L_3 EXAFS k^3 weighted spectra (k min = 3, k max = 9.5 in M. sativa and *M. vulgare*; k min = 3 and k max = 9.0 in *M. vulgare* spot) are presented.

hydroponically[21,26,38,39] and in most plants growing in Hg-polluted soils.[25,40] However, the exact localization of Hg in root tissues, and the binding mechanism that enables this high accumulation are still undetermined.

Mercury in Hydroponically Grown *M. sativa*. Mercury accumulated at the apex of secondary and primary roots of *M. sativa* treated with 30 μM Hg (Figure 1), as was found for *Spartina* spp. plants.[18] However, root response was not immediate; after 5 h, Hg could be detected at all parts of the root tip (part A of Figure 1), but after a longer exposure (1 to 7 days, parts B and C of Figure 1) the root cap contained less Hg (marked with pink arrows) implying significant change at this region due to the exposure to Hg. With longer exposure, Hg continued to accumulate in young tissues just behind the meristematic zones (parts C and D of Figure 1) and translocated up via the vascular cylinder, with a minor Hg-signal at the epidermis (part D of Figure 1). The latter observation is in agreement with the distribution described previously in primary mature alfalfa root.[19] It appears that the cells just behind the apical meristem are not well differentiated, less suberized, and thus more permeable to water and solutes[41] facilitating the movement of ions such as Hg^{2+} into the root. The suberized Casparian strip at the endodermis of mature roots constitutes a barrier to the apoplastic free diffusion of water and solutes, which are forced to enter the root symplast prior to xylem loading.[42] It has been found that the appearance of such apoplastic barriers determines the rate of uptake and movement of Cd in maize plants, which was higher in immature root regions (i.e., root apex, ref 43). This might explain the rapid and strong increase of Hg signal at the root apex found in alfalfa (parts A−C of Figure 1), where most Hg would enter the plant via apoplast rather than via symplast at the mature zone (part D of Figure 1).

TEM imaging of Hg-treated root sections showed high-density metal deposits at the intercellular spaces attached to the epidermal cells (parts B and C of Figure 2), in agreement with Hg accumulation sites found by μ-SXRF (part D of Figure 1). The high deposits in the endodermis cells (part F of Figure 2), also fit with the localization of Hg previously observed by μ-tomography X-ray fluorescence of *M. sativa* root.[19] The distribution inside the endodermal cells might indicate penetration into the symplast. Interestingly, high density stains were also observed in cell walls of the cortical parenchyma (part E of Figure 2) and strengthened in xylem cells (parts F and J of Figure 2). The latter finding matched the strong signal of Hg detected at the vascular cylinder by μ-SXRF (part D of Figure 1) and by μ-tomography X-ray Fluorescence of *M. sativa* root.[19] Similar distribution was also described for Cd in carrot roots, accumulated as electron-dense deposits in the intercellular spaces of cortical and xylem cell walls,[33] but in contrast to those findings no vacuolar deposits could be detected in Hg-treated plants (Figure 2). It should be noted that the sensitivity of both techniques (TEM or μ-SXRF) is relatively low; thus, low concentrations or diffused Hg-complexes (such as Hg−PCs) might be missed. However, the preferred localization of Hg observed at the cell wall coincides with earlier studies that found by subcellular fractionation that up to 90% of total Hg was associated with root cell walls of *Halimione portulacoides*,[23] maize, barley, and alfalfa plants,[19] and a variety of marsh plants.[44] A criticism is sometimes made toward these subcellular fractionation methods questioning their ability to maintain the integrity of sucellular organs; in this study we reinforced their findings using a different method.

Cell walls are often considered an important sink for metals, and a possible defense mechanism,[13] as suggested for Cd,[45] Pb,[46] and Cu.[47] The storage mechanisms differed with metal type and plant species, including precipitation in cell walls and binding to cell wall components. The binding usually involved oxygen containing ligands, such as hydroxyl and carboxyl groups, which are abundant in cell wall components (cellulose, hemicelluloses, pectin, and lignin). In contrast, according to our EXAFS spectra, the great majority of Hg in roots of *M. sativa* was bound to sulfur in thiol groups (Table 2). Hence, potential binding sites in cell walls would be structural proteins, such as extensins[48,49] and expansins,[50,51] which contain characteristic cysteine-rich regions. Thiol groups in cysteine residues often have a critical role supporting the spatial structure of the proteins; strong binding of Hg to these groups is expected to impair their functionality and subsequently the functioning and structure of cell walls. This might explain the observed deformation found in epidermal and cortical cells and especially the abnormal thickening and faults in xylem cells of Hg-treated alfalfa roots (Figure 2). The high expression of these proteins in xylem cells[48,51] coincides with the high Hg accumulation observed in vascular tissues by μ-SXRF (Figure 1) and TEM (parts F and J of Figure 2). However, Hg binding to plasma membrane proteins such as aquaporins,[52] which hinders water movement into cells, may also contribute to the observed phenomena.

Another important portion of organic Hg−S is phytochelatins (PCs), found as an array of phytochelatins (PCs) in different plant species.[19,53,54] We have attempted to determine the contribution of Hg−PCs complexes to the Hg−S fraction by EXAFS analysis using different reference compounds, but we could not differentiate unequivocally between the different types of biothiols or proteins in these heterogeneous vegetal

samples. Though the LSF results were significantly improved by the combination of Hg−PC and Hg−Cys (as given in Table 2), an absolute identification of the exact compounds will require the use of complementary methods. Recent studies have shown that PCs have the ability to undergo long-distance transport in the root-to-shoot and shoot-to-root directions and might be involved in long distance metal transport.[55,56] Indeed, μ-SXRF showed that Hg was translocated through the vascular tissues from root to stems and leaves, where it was distributed through veins (parts D, F, and H of Figure 1). The major Hg form in the stem fitted well with that of Hg−PC suggesting that Hg is carried up to the leaves by similar soluble thiols. Translocation from root to shoot is often considered an inefficient process (<5%),[57−59] compared to direct absorption of Hg by leaves. Yet, our results clearly show that under the examined conditions (hydroponic system and high concentrations), uptake by roots appeared to supply the major fraction of Hg in leaves (note Hg concentration in control leaves in Table 1; exposed to the same air conditions as treated plants).

In this study, we found significant concentrations of methylated Hg (CH_3−Hg) in roots and leaves (Table 2) as was found previously in roots of hydroponically grown *M. sativa*.[19] This toxic form is a byproduct of bacterial activity in aquatic systems[60] and appeared to be produced in the hydroponic growth solution as well. We could not determine the specific effects of each Hg-species in the present setup.

Mercury in Field Samples of *M. vulgare* Plants. The distribution and speciation of Hg in the roots of naturally occurring *M. vulgare* plants, collected from a contaminated site in Almadén, was different from that of the hydroponically grown *M. sativa*. The concentration of Hg in plants increased with Hg soil levels, as reported by Millán et al.[28] Still it was 1 order of magnitude lower than the concentration measured in the roots of *M. sativa*. μ-SXRF analysis of root cross sections detected Hg-signal mainly at the outer layer (part B of Figure 4). The elemental composition and the high heterogeneity detected by μ-SXRF in this region of the root (data not shown) imply significant contribution of soil components to the measured concentration of Hg. Indeed, the bulk EXAFS analysis of *M. vulgare* roots and leaves revealed that a high percentage (58−83%, Table 2) of total Hg was composed of HgS minerals (cinnabar Hg−S red, and metacinnabar Hg−S black), which are the major Hg species found in the surrounding soils.[27] We could identify an intrusion of this heterogeneous external layer into the inner parts of the root (arrow in part B of Figure 4) resulting in bright spots corresponding to high Hg concentrations. To clarify their identity, we used a μ-EXAFS probe on a bright spot shown in parts B and C of Figure 4 (marked with number 1) and confirmed that it fit well with the Hg mineral cinnabar (part C of Figure 3). It appears that a significant fraction of Hg in field samples could result from deposition of soil microparticles in roots and shoots in spite of intensive cleaning procedures. Interestingly, a minor proportion of Hg in the shoot corresponded to Hg−biothiol/proteins according to LSF analysis implying that a certain amount of Hg was actually assimilated by the plants (Table 2).

To sum up, the presented results were obtained in plants grown hydroponically or collected in Hg-polluted soil using the same analytical methods. The concentrations of the different Hg species in *M. sativa* and *M. vulgare* are summarized in Figure S4 of the Supporting Information calculated from the data of Hg concentration in each organ (Table 1) and its relative abundance as determined by LSF using the L_3 EXAFS k^3 spectra (Table 2). The enhanced translocation to leaves in the hydroponic system might be associated with root architecture with fewer apoplastic barriers (i.e., less suberized Casparian strips) compared to plants grown in polluted soils with enhanced apoplastic barriers.[43] In spite of the big differences in Hg concentration between the roots of the examined plants, the total fraction of Hg associated with biothiols and/or proteins (i.e., metabolically processed Hg) in the leaves of both species was on the same order of magnitude (Figure S4 of the Supporting Information). This resemblance might indicate similar mechanisms of detoxification or a limiting factor for S-organic binding in leaves. In contrast, the storage capacity for Hg in roots appears to be very flexible, resulting in significant differences (2 orders of magnitude) between examined plants. Obviously, further analysis must be carried out in order to understand the exact mechanisms involved in Hg uptake and translocation under a variety of conditions and in different plant species.

The results presented could be utilized to select plants with enhanced capability to retain Hg in below-ground organs, to optimize phytostabilization strategies for heavily Hg-polluted soils. Thus, plants could be selected with specific traits such as highly suberized roots (barriers limiting Hg apoplastic movement) or with higher binding capacity to cell wall materials (as suggested above for structural proteins).

■ ASSOCIATED CONTENT

Ⓢ Supporting Information

Growth conditions, detailed description of samples preparation, technical data, details of the field site, and figures relating to data analysis. This material is available free of charge via the Internet at http://pubs.acs.org.

■ AUTHOR INFORMATION

Corresponding Author

*Phone: 00 34 914976323, fax: 34 914978344, e-mail: sandra.carrasco.gil@eead.csic.es.

Present Address

¶The Jacob Blaustein Institutes for Desert Research, Ben-Gurion University of the Negev, Sede Boqer Campus, Midreshet Ben-Gurion, 84990 Israel.

Author Contributions

†S.C.G. and H.S. contributed equally to this work.

Notes

The authors declare no competing financial interest.

■ ACKNOWLEDGMENTS

This work was supported by Fundación Ramón Areces, the Spanish Ministry of Science and Innovation (AGL2010-15151-PROBIOMET and CTM2005-04809/TECNO-REUSA), and Junta Comunidades Castilla-La Mancha (FITOALMA2, POII10-0087-6458). The Vaadia Postdoctoral Fellowship Award (FI-405-2007) from the United States-Israel Binational Agricultural Research and Development Fund. Portions of this research were carried out at the Stanford Synchrotron Radiation Lightsource, a Directorate of SLAC National Accelerator Laboratory and an Office of Science User Facility operated for the U.S. Department of Energy Office of Science by Stanford University. The contents of this publication are solely the responsibility of the authors and do not necessarily represent the official views of NIGMS, NCRR or NIH. We

highly thank Prof Gordon Brown of Stanford University for his advice and for the use of his lab facilities. We thank MJ Sierra and MT Villadoniga for helping in the *M. vulgare* sample collection and W Amos and J Cassano for their help with data collection. We also thank MAYASA for allowing the collection of soil and plant samples in Hg contaminated sites of the Almadén mining area.

REFERENCES

(1) Options for reducing mercury used in products and applications, and the fate of mercury already circulating in Society; Contract: ENV.G.2/ETU/2007/0021; European Commission, 2008; http://ec.europa.eu/environment/chemicals/mercury/pdf/study_report2008.pdf

(2) Higueras, P.; Oyarzun, R..; Munha, J.; Morata, D. Palaeozoic magmatic-related hydrothermal activity in the Almadén syncline, Spain: a long-lasting Silurian to Devonian process? *Transactions of the Institution of Mining and Metallurgy Section B-Applied Earth Science* **2000**, *109*, 199−202.

(3) W.H.O.. Ernst. *Chemie Erde Geochem.* **2005**, *65*, 29−42.

(4) Higueras, P.; Oyarzun, R.; Biester, H.; Lillo, J.; Lorenzo, S. A first insight into mercury distribution and speciation in soils from the Almadén mining district, Spain. *J. Geochem. Explor.* **2003**, *80* (1), 95−104.

(5) Clarkson, T. W. The biological properties and distribution of mercury. *Biochem. J.* **1972**, *130*, 61−63.

(6) Boening, D. W. Ecological effects, transport, and fate of mercury: A general review. *Chemosphere* **2000**, *40* (12), 1335−1351.

(7) Baldi, F. Microbial transformation of mercury species and their importance in the biogeochemical cycle of Hg. In *Mercury and its Effects on Environment and Biology*; Sigel, H., Sigel, A., Eds.; Marcell Dekker, Inc: New York, 1997; pp 213.

(8) Feng, X.; Li, P.; Qiu, G.; Wang, S.; Li, G.; Shang, L.; Meng, B.; Jiang, H.; Bai, W.; Li, Z.; Fu, X. Human exposure to methylmercury through rice intake in mercury mining areas, Guizhou province, China. *Environ. Sci. Technol.* **2008**, *42* (1), 326−332.

(9) Zhang, H.; Feng, X.; Larssen, T.; Qiu, G.; Vogt, R. D. In inland China, rice, rather than fish, is the major pathway for methylmercury exposure. *Environ. Health Perspect.* **2010**, *118* (9), 1183−1188.

(10) Arruda, M. A. Z.; Azevedo, R. A. Metallomics and chemical speciation: Towards a better understanding of metal-induced stress in plants. *Annals of Applied Biology* **2009**, *155* (3), 301−307.

(11) Punshon, T.; Guerinot, M. L.; Lanzirotti, A. Using synchrotron X-ray fluorescence microprobes in the study of metal homeostasis in plants. *Annals of Botany* **2009**, *103*, 665−672.

(12) Mendez, M. O.; Maier, R. M. Phytoremediation of mine tailings in temperate and arid environments. *Reviews in Environmental Science and Biotechnology* **2008**, *7*, 47−59.

(13) Hall, J. L. Cellular mechanisms for heavy metal detoxification and tolerance. *J. Experimental Botany* **2002**, *52*, 631−640.

(14) Donner, E.; Punshon, T.; Guerinot, M. L.; Lombi, E. Functional characterisation of metal(loid) processes in planta through the integration of synchrotron techniques and plant molecular biology. *Anal. Bioanal. Chem.* **2012**, *402* (10), 3287−3298.

(15) Kopittke, P. M.; de Jonge, M. D.; Menzies, N. W.; Wang, P.; Donner, E.; McKenna, B. A.; Paterson, D.; Howard, D. L.; Lombi, E. Examination of the distribution of arsenic in hydrated and fresh cowpearoots using two- and three-dimensional techniques. *Plant Physiology* **2012**, *159* (3), 1149−1158.

(16) Lombi, E.; Scheckel, K. G.; Kempson, I. M. In situ analysis of metal(loid)s in plants: State of the art and artefacts. *Environmental and Experimental Botany* **2011**, *72* (1), 3−17.

(17) De Filippis, L. F.; Pallaghy, C. K. Localization of zinc and mercury in plant cells. *Micron* **1975**, *6*, 111−120.

(18) Patty, C.; Barnett, B.; Mooney, B.; Kahn, A.; Levy, S.; Liu, Y. J.; Pianetta, P.; Andrews, J. C. Using X-ray microscopy and Hg L-3 XANES to study Hg binding in the rhizosphere of Spartina cordgrass. *Environ. Sci. Technol.* **2009**, *43* (19), 7397−7402.

(19) Carrasco-Gil, S.; Álvarez-Fernández, A.; Sobrino-Plata, J.; Millán, R.; Carpena-Ruiz, R. O.; LeDuc, D. L.; Andrews, J. C.; Abadía, J.; Hernández, L. E. Complexation of Hg with phytochelatins is important for plant Hg tolerance. *Plant, Cell and Environment* **2011**, *34*, 778−791.

(20) Siebner H., Wang Y., Newville M., Andrews J. C., and Brown Jr. G. E., Distribution and transformation of mercury in plant roots at the abandoned mercury mine site, New Idria, CA. In 11th International Conference on the Biogeochemistry of Trace Elements: Florence, Italy, 2011.

(21) Riddle, S. G.; Tran, H. H.; Dewitt, J. G.; Andrews, J. C. Field, laboratory, and X-ray absorption spectroscopic studies of mercury accumulation by water hyacinths. *Environ. Sci. Technol.* **2002**, *36*, 1965−1970.

(22) Rajan, M.; Darrow, J.; Hua, M.; Barnett, B.; Mendoza, M.; Greenfield, B. K.; Andrews, J. C. Hg L-3 XANES study of mercury methylation in shredded Eichhornia crassipes. *Environ. Sci. Technol.* **2008**, *42* (15), 5568−5573.

(23) Valega, M.; Lima, A. I. G.; Figueira, E.; Pereira, E.; Pardal, M. A.; Duarte, A. C. Mercury intracellular partitioning and chelation in a salt marsh plant, *Halimione portulacoides (L.) Aellen*: Strategies underlying tolerance in environmental exposure. *Chemosphere* **2009**, *74* (4), 530−536.

(24) Moreno-Jiménez, E.; Gamarra, R.; Carpena-Ruiz, R. O.; Millán, R.; Peñalosa, J. M.; Esteban, E. Mercury bioaccumulation and phytotoxicity in two wild plant species of Almadén area. *Chemosphere* **2006**, *63* (11), 1969−1973.

(25) Millán, R.; Gamarra, R.; Schmid, T.; Sierra, M. J.; Quejido, A. J.; Sánchez, D. M.; Cardona, A. I.; Fernández, M.; Vera, R. Mercury content in vegetation and soils of the Almadén mining area (Spain). *Science of The Total Environment* **2006**, *368* (1), 79−87.

(26) Ortega-Villasante, C.; Rellan-Alvarez, R.; Del Campo, F. F.; Carpena-Ruiz, R. O.; Hernandez, L. E. Cellular damage induced by cadmium and mercury in Medicago sativa. *J. Experimental Botany* **2005**, *56* (418), 2239−2251.

(27) Esbrí, J. M.; Bernaus, A.; Ávila, M.; Kocman, D.; García-Noguero, E. M.; Guerrero, B.; Gaona, X.; Álvarez, R.; Perez-Gonzalez, G.; Valiente, M.; Higueras, P.; Horvat, M.; Loredo, J. XANES speciation of mercury in three mining districts − Almadén, Asturias (Spain), Idria (Slovenia). *J. Synchrotron Radiat.* **2010**, *17* (2), 179−186.

(28) Millan, R.; Schmid, T.; Sierra, M. J.; Carrasco-Gil, S.; Villadóniga, M.; Rico, C.; Ledesma, D. M. S.; Puente, F. J. D. Spatial variation of biological and pedological properties in an area affected by a metallurgical mercury plant: Almadenejos (Spain). *Appl. Geochem.* **2011**, *26*, 174−181.

(29) Gustafsson J. P. Software and documentation available at http://www2.lwr.kth.se/English/OurSoftware/vminteq

(30) Ortega-Villasante, C.; Hernandez, L. E.; Rellan-Alvarez, R.; Del Campo, F. F.; Carpena-Ruiz, R. O. Rapid alteration of celular redox homeostasis upon exposure to cadmium and mercury in alfalfa seedlings. *New Phytologist* **2007**, *176* (1), 96−107.

(31) Webb, S. Software and documentation available at http://www..stanford.edu/~swebb (accessed February 26, 2009).

(32) Russin, W. A., Trivett, C. L. Vacuum-Microwave combination for processing plant tissues for electron microscopy. In *Microwave Techniques and Protocols*; Giberson, R. T., Demaree Jr R. S., Eds.; Totowa: Humana Press 2001; pp 25−34.

(33) Sanità di Toppi, L.; Vurro, E.; De Benedictis, M.; Falasca, G.; Zanella, L.; Musetti, R.; Lenucci, M. S.; Dalessandro, G.; Altamura, M. M. A bifasic response to cadmium stress in carrot: Early acclimatory mechanisms give way to root collapse further to prolonged metal exposure. *Plant Physiology and Biochemistry* **2012**, *58* (0), 269−279.

(34) Webb, S. M. Sixpack: A graphical user interface for XAS analysis using IFEEF IT. *Phys. Scr.* **2005**, *115*, 1011−1014.

(35) Kim, C. S.; Brown, G. E.; Rytuba, J. J. Characterization and speciation of mercury-bearing mine wastes using X-ray absorption spectroscopy. *Sci. Total Environ.* **2000**, *261* (1−3), 157−168.

(36) Kelly, S. D.; et al. Analysis of Soils and Minerals Using X-ray Absorption Spectroscopy. In *Methods of Soil Analysis, Part 5 -Mineralogical Methods*; Ulery, A. L., Drees, L. R., Eds.; Soil Science Society of America: Madison, 2008; pp 367.
(37) Martinez-Coronado, A.; Oyarzun, R.; Esbri, J. M.; Llanos, W.; Higueras, P. Sampling high to extremely high Hg concentrations at the Cerco de Almadenejos, Almaden mining district (Spain): The old metallurgical precinct (1794 to 1861 AD) and surrounding areas. *Journal of Geochemical Exploration* **2011**, *109* (1−3), 70−77.
(38) Rellan-Alvarez, R.; Ortega-Villasante, C.; Alvarez-Fernandez, A.; del Campo, F. F.; Hernandez, L. E. Stress responses of *Zea mays* to cadmium and mercury. *Plant and Soil* **2006**, *279* (1−2), 41−50.
(39) Esteban, E.; Moreno, E.; Peñalosa, J.; Cabrero, J. I.; Millán, R.; Zornoza, P. Short and long-term uptake of Hg in white lupin plants: Kinetics and stress indicators. *Environmental and Experimental Botany* **2008**, *62* (3), 316−322.
(40) Sierra, M. J.; Millán, R.; Esteban, E. Mercury uptake and distribution in Lavandula stoechas plants grown in soil from Almadén mining district (Spain). *Food Chem. Toxicol.* **2009**, *47* (11), 2761−2767.
(41) Hose, E.; Clarkson, D. T.; Steudle, E.; Schreiber, L.; Hartung, W. The exodermis: A variable apoplastic barrier. *Journal of Experimental Botany* **2001**, *52* (365), 2245−2264.
(42) Tester, M.; Leigh, R. A. Partitioning of nutrient transport processes in roots. *J. Experimental Botany* **2001**, *52*, 445−457.
(43) Redjala, T.; Zelko, I.; Sterckeman, T.; Legue, V.; Lux, A. Relationship between root structure and root cadmium uptake in maize. *Environmental and Experimental Botany* **2011**, *71* (2), 241−248.
(44) Castro, R.; Pereira, S.; Lima, A.; Corticeiro, S.; Valega, M.; Pereira, E.; Duarte, A.; Figueira, E. Accumulation, distribution and cellular partitioning of mercury in several halophytes of a contaminated salt marsh. *Chemosphere* **2009**, *76* (10), 1348−1355.
(45) LozanoRodriguez, E.; Hernandez, L. E.; Bonay, P.; CarpenaRuiz, R. O. Distribution of cadmium in shoot and root tissues of maize and pea plants: Physiological disturbances. *J. Experimental Botany* **1997**, *48* (306), 123−128.
(46) Tian, S.; Lu, L.; Yang, X.; Webb, S. M.; Du, Y.; Brown, P. H. Spatial imaging and speciation of lead in the accumulator plant *Sedum alfedii* by microscopically focused synchrotron X-ray investigation. *Environ. Sci. Technol.* **2010**, *44* (15), 5920−5926.
(47) Kopittke, P. M.; Menzies, N. W.; de Jonge, M. D.; McKenna, B. A.; Donner, E.; Webb, R. I.; Paterson, D. J.; Howard, D. L.; Ryan, C. G.; Glover, C. J.; Scheckel, K. G.; Lombi, E. In situ distribution and speciation of toxic copper, nickel, and zinc in hydrated roots of cowpea. *Plant Physiology* **2011**, *156* (2), 663−673.
(48) Baumberger, N.; Doesseger, B.; Guyot, R.; Diet, A.; Parsons, R. L.; Clark, M. A.; Simmons, M. P.; Bedinger, P.; Goff, S. A.; Ringli, C.; Keller, B. Whole-genome comparison of leucine-rich repeat extensins in Arabidopsis and rice. A conserved family of cell wall proteins form a vegetative and a reproductive clade. *Plant Physiology* **2003**, *131* (3), 1313−1326.
(49) Ringli, C. The role of extracellular LRR-extensin (LRX) proteins in cell wall formation. *Plant Biosystems* **2005**, *139* (1), 32−35.
(50) Darley, C. P.; Forrester, A. M.; McQueen-Mason, S. J. The molecular basis of plant cell wall extension. *Plant Molecular Biology* **2001**, *47* (1−2), 179−195.
(51) Im, K. H.; Cosgrove, D. J.; Jones, A. M. Subcellular localization of expansin mRNA in xylem cells. *Plant Physiology* **2000**, *123* (2), 463−470.
(52) Zhang, W. H.; Tyerman, S. D. Inhibition of water channels by $HgCl_2$ in intact wheat root cells. *Plant Physiology* **1999**, *120* (3), 849−857.
(53) Chen, L.; Yang, L.; Wang, Q. In vivo phytochelatins and Hg-phytochelatin complexes in Hg-stressed *Brassica chinensis L. Metallomics* **2009**, *1* (1), 101−106.
(54) Krupp, E. M.; Mestrot, A.; Wielgus, J.; Meharg, A. A.; Feldmann, J. The molecular form of mercury in biota: identification of novel mercury peptide complexes in plants. *Chem. Commun.* **2009**, *28*, 4257−4259.
(55) Chen, X. Y.; Kim, J. Y. Transport of macromolecules through plasmodesmata and the phloem. *Physiologia Plantarium* **2006**, *126*, 560−571.
(56) Gong, J. M.; Lee, D. A.; Schroeder, J. I. Long-distance root-to-shoot transport of phytochelatins and cadmium in *Arabidopsis*. *Proc. Natl. Acad. Sci. U.S.A.* **2003**, *100*, 10118−10123.
(57) Lindberg, S. E.; Jackson, D. R.; Huckabee, J. W.; Janzen, S. A.; Levin, M. J.; Lund, J. R. Atmospheric emmission and plant uptake of mercury from agricultural soils near the Almadén mercury mine. *J. Environ. Qual.* **1979**, *8*, 572−578.
(58) Mosbaek, H.; Tjell, J. C.; Sevel, T. Plant uptake of airborne mercury in backgrouns areas. *Chemosphere* **1988**, *17*, 1227−1236.
(59) Ericksen, J. A.; Gustin, M. S.; Schorran, D. E.; Johnson, D. W.; Lindberg, S. E.; Coleman, J. S. Accumulation of atmospheric mercury in forest foliage. *Atmos. Environ.* **2003**, *37*, 1613−1622.
(60) Benoit, J. M.; Gilmour, C. C.; Heyes, A.; Mason, R. P.; Miller, C. L., Geochemical and biological controls over methylmercury production and degradation in aquatic ecosystems. In *Biogeochemistry of Environmentally Important Trace Elements*; Cai, Y. B. O. C., Ed.; **2003**; Vol. *835*, pp 262-297.